

**MAIN TEXT**

# Magnetic resonance imaging during warm ex vivo kidney perfusion

Rianne Schutter<sup>1</sup>  | Otis C. van Varsseveld<sup>1</sup> | Veerle A. Lantinga<sup>1</sup>  |  
 Merel B. F. Pool<sup>1</sup> | Tim H. Hamelink<sup>1</sup> | Jan Hendrik Potze<sup>2</sup> |  
 Henri G. D. Leuvenink<sup>1</sup> | Christoffer Laustsen<sup>3</sup>  | Ronald J. H. Borra<sup>2</sup> | Cyril Moers<sup>1</sup>

<sup>1</sup>Department of Surgery – Organ Donation and Transplantation, University Medical Center Groningen, University of Groningen, Groningen, The Netherlands

<sup>2</sup>Department of Radiology, University Medical Center Groningen, University of Groningen, Groningen, The Netherlands

<sup>3</sup>Department of Clinical Medicine, The MR Research Center, Aarhus University, Aarhus, Denmark

**Correspondence**

Rianne Schutter, Department of Surgery – Organ Donation and Transplantation, Room R4.202, Internal post code BA11, Hanzeplein 1, 9713 GZ Groningen, The Netherlands.  
 Email: [r.schutter@umcg.nl](mailto:r.schutter@umcg.nl)

**Funding information**

H2020 European Research Council, Grant/Award Number: 851368 - PRE-IMAGE; Nierstichting, Grant/Award Number: 17OI01

**Abstract**

**Background:** The shortage of donor organs for transplantation remains a worldwide problem. The utilization of suboptimal deceased donors enlarges the pool of potential organs, yet consequently, clinicians face the difficult decision of whether these sub-optimal organs are of sufficient quality for transplantation. Novel technologies could play a pivotal role in making pre-transplant organ assessment more objective and reliable.

**Methods:** Ex vivo normothermic machine perfusion (NMP) at temperatures around 35–37°C allows organ quality assessment in a near-physiological environment. Advanced magnetic resonance imaging (MRI) techniques convey unique information about an organ's structural and functional integrity. The concept of applying magnetic resonance imaging during renal normothermic machine perfusion is novel in both renal and radiological research and we have developed the first MRI-compatible NMP setup for human-sized kidneys.

**Results:** We were able to obtain a detailed and real-time view of ongoing processes *inside* renal grafts during ex vivo perfusion. This new technique can visualize structural abnormalities, quantify regional flow distribution, renal metabolism, and local oxygen availability, and track the distribution of ex vivo administered cellular therapy.

**Conclusion:** This platform allows for advanced pre-transplant organ assessment, provides a new realistic tool for studies into renal physiology and metabolism, and may facilitate therapeutic tracing of pharmacological and cellular interventions to an isolated kidney.

**KEYWORDS**

kidney transplantation, magnetic resonance imaging, renal physiology

Otis C. van Varsseveld and Veerle A. Lantinga contributed equally.

This is an open access article under the terms of the [Creative Commons Attribution-NonCommercial-NoDerivs](https://creativecommons.org/licenses/by-nc-nd/4.0/) License, which permits use and distribution in any medium, provided the original work is properly cited, the use is non-commercial and no modifications or adaptations are made.

© 2022 The Authors. *Artificial Organs* published by International Center for Artificial Organ and Transplantation (ICAOT) and Wiley Periodicals LLC.



## 1 | INTRODUCTION

### 1.1 | Quality assessment of donor organs

End-stage organ failure has a major impact on the well-being of affected patients. Successful organ transplantation results in improved health-related quality of life.<sup>1–4</sup> Alongside the merits of transplantation, society continues to encounter a serious problem: the shortage of available donor organs suitable for transplantation. The increased use of deceased donors of advanced age and with substantial comorbidities enlarges the pool of potential organs. Yet, as a consequence, clinicians progressively face the difficult decision of whether these sub-optimal organs are suitable for transplantation. Reasons to decline donor organs are diverse, depending on local protocols as well as clinicians' individual preferences, and differ for each type of organ, but are mostly associated with presumed inferior organ quality. Organ quality assessment is currently based on clinical judgment and remains predominantly subjective, hence organs suitable for transplantation could be inappropriately discarded. Conversely, around 24% of transplanted kidneys that have been retrieved from older-age donors do not show acceptable outcomes within 1-year post-transplant.<sup>5</sup> Novel technologies could play a pivotal role in making pre-transplant donor organ assessment more objective and reliable.

### 1.2 | Machine perfusion

Ex vivo machine perfusion technologies are gaining popularity as they may allow for better organ preservation, viability assessment, and organ re-conditioning prior to transplantation.<sup>6</sup> Hypothermic (1–7°C) machine perfusion prior to transplantation has earned its place as a superior modality for donor kidney preservation compared to static cooling.<sup>7</sup> Ex vivo *normothermic* machine perfusion (NMP) at temperatures around 35–37°C entails further advantages, such as organ quality assessment in a near-physiological environment and the opportunity to administer therapy to an isolated organ before transplantation. Despite the growing number of transplant centers adopting clinical NMP technology, there is still a lack of knowledge about which markers and criteria define the quality of a kidney. Novel methods such as advanced organ imaging could play a pivotal role, as this technique can provide a better understanding of how physiological and metabolic conditions on a regional level *within* the organ evolve over time *during* ex vivo perfusion, and how these differ from in vivo circumstances.

### 1.3 | Magnetic resonance imaging of ex vivo perfused kidneys

Magnetic resonance imaging (MRI) techniques have rapidly advanced in recent years, resulting in sophisticated imaging sequences that likely convey unique information about organ viability. In 2007, Buchs et al. described the first case of an MRI-compatible hypothermic perfusion setup.<sup>8</sup> With their model, an MRI evaluation of ischaemically injured porcine kidneys during cold oxygenated machine perfusion could be performed. Nevertheless, renal metabolism is eminently reduced under hypothermic conditions, which limits relevant organ quality assessment. The near-physiological conditions offered by NMP provide a more suitable platform for MRI evaluation of ex vivo donor kidneys.

With this promising application in mind, our group set out to develop the first MRI-compatible ex vivo NMP setup for human-sized kidneys. We aimed to obtain a detailed view of ongoing processes *inside* human-sized kidneys during normothermic ex vivo perfusion and gain insight into the functional regional differences within the kidney.

## 2 | MATERIALS AND METHODS

### 2.1 | Porcine kidneys

Normothermic ex vivo perfusions in the Netherlands were performed with viable porcine kidneys ( $n = 22$ ) procured from a local slaughterhouse (Kroon Vlees, Groningen, the Netherlands) by the guidelines of the Dutch food safety authority according to standard slaughterhouse procedures. Approximately, 20 min after the circulatory arrest of the pig, kidneys were procured and the kidney with the most favorable vasculature was connected to a pressure-controlled led oxygenated hypothermic machine perfusion (HMP) device (Kidney Assist Transport®, Organ Assist B.V, Groningen, the Netherlands) primed with cold (1–5°C) University of Wisconsin Machine Perfusion Solution (Belzer MPS®, Bridge to Life, Columbia, USA) and set at a perfusion pressure of 25 mmHg. HMP was used to bridge the time interval between organ retrieval in the early morning and the availability of the MRI scanner in the evening, mimicking a clinically realistic cold organ preservation interval of approximately 10 h.

The experiments with magnetic resonance spectroscopy ( $n = 4$ ) were performed in another facility, and organ retrieval and the perfusion setup were slightly different. Kidneys ( $131 \pm 5$  g) were procured from female Danish domestic pigs ( $40 \pm 2$  kg). All experiments were performed by Danish legislation and were approved by the Danish Animal Experiments Inspectorate. After nephrectomy



under anesthesia, kidneys were flushed with 1 L of 4°C heparinized ringer acetate (Fresenius Kabi, Bad Homburg, Germany), and the renal artery and ureter were cannulated before the kidney was stored in a 4°C ringer acetate filled transport bag. Ex vivo perfusion of the kidney started after  $32 \pm 6$  min of static cold storage.

## 2.2 | Discarded human kidneys

Human discarded kidneys were obtained once a kidney of a deceased donor in the Netherlands was rejected by all centers within the Eurotransplant region. Permission was requested from the donors' relatives, and written consent was obtained. These human donor kidneys had not been accepted for transplantation because of either suspected malignancy in the iliac lymph nodes, positive hepatitis B virology (2 kidneys from 1 donor), or small kidney size with multiple cysts and thus became available for research. Because of the non-elective nature of logistics surrounding the procurement of human donor kidneys, warm and cold ischemia times before the start of NMP could not be protocolled and were diverse. Two kidneys in our group of four underwent static storage on ice and two kidneys were connected to a clinical HMP device after retrieval.

## 2.3 | Ex vivo normothermic perfusion setup

Our MRI-compatible NMP setup in the Netherlands (Figure 1) is described in detail in the online supplement section. The perfusion solution for porcine kidneys conducted in the Netherlands consisted of autologous red blood cells (RBCs), crystalloids, albumin, creatinine, antibiotics, and electrolyte supplementation (Supporting Information Table 3). For human kidney perfusions, human-packed red blood cells, type O negative, were provided by our transfusion laboratory. The perfusion solution was oxygenated with 0.5 L/min carbogen gas, (95% O<sub>2</sub> + 5% CO<sub>2</sub>) and kept at 35–37°C with continuous pressure of 85 mm Hg.

## 2.4 | MRI protocol

Imaging sequences were mainly performed on 3T Magnetom Prisma (software-platform VE-11C) and some on 3T Magnetom Skyra (Siemens Healthineers, Erlangen, Germany) clinical MRI scanners. An overview of essential imaging acquisition parameters is available in the online Supporting Information.

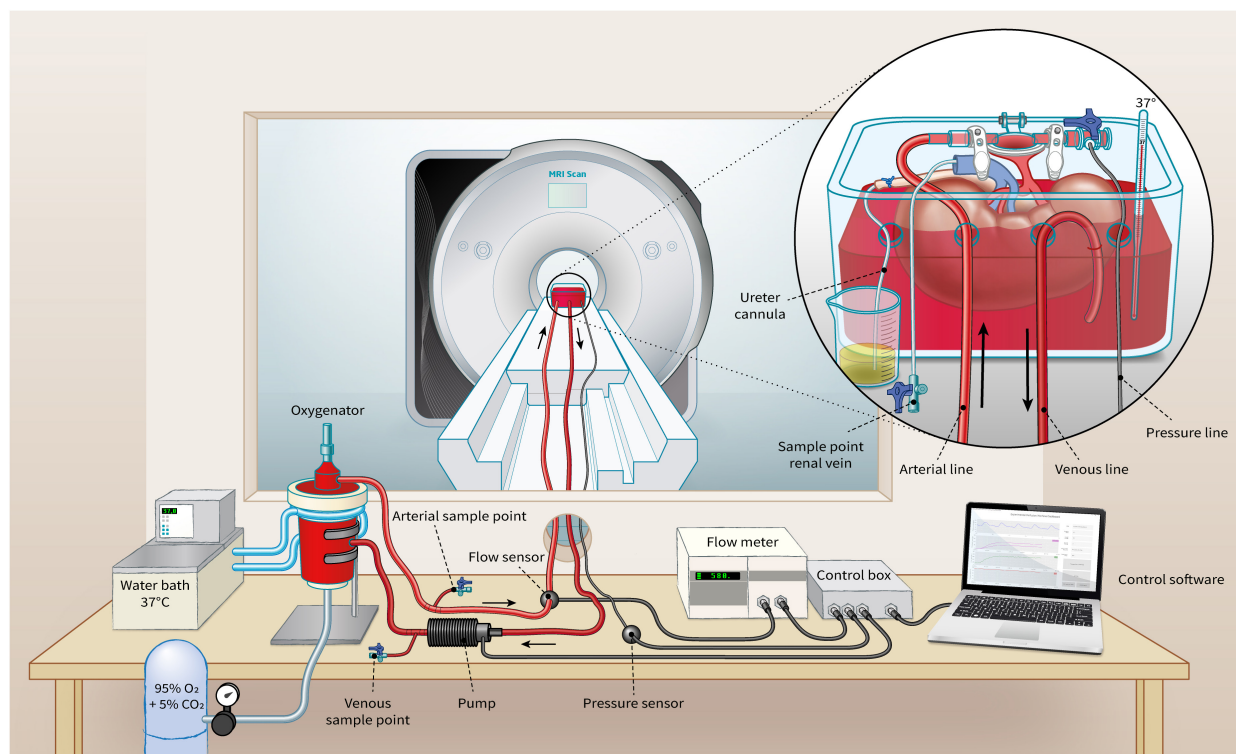


FIGURE 1 Schematic impression of our MRI-compatible setup for ex vivo normothermic kidney perfusion [Color figure can be viewed at [wileyonlinelibrary.com](http://wileyonlinelibrary.com)]



### 3 | RESULTS

Between April 2016 and October 2020, 26 porcine and four human discarded kidneys were evaluated on our MRI-compatible setup for ex vivo normothermic perfusion. Our results derive from an early pilot phase in which a wide variety of classic and novel imaging sequences were performed, followed by a standardized perfusion and imaging protocol with a duration of at least 3 h, and several experiments with a specific focus on ischemia-reperfusion or with labeled particles (Table 1).

#### 3.1 | Structural imaging

Anatomical T2-weighted imaging allowed detailed non-invasive visualization of inner structural anomalies of the kidney, showing fat and water as areas with a high signal. Renal abnormalities encountered in the experiments with porcine kidneys included a parenchymal cyst, a large subcapsular hematoma, and hydronephrosis of iatrogenic origin (Figure 2A–C). The benign cystic structure was discovered in our images and could not be detected by visual inspection of the kidney's exterior. In another case, we observed an acute onset of reduced renal blood flow with increased vascular resistance. Diagnostic T2-weighted imaging revealed an acutely arisen subcapsular hematoma compressing part of the renal parenchyma and vascular structures. After external decompression of the

hematoma, all perfusion parameters returned to normal values. During a subsequent experiment, urine production was absent during the first 30 min of NMP. Imaging showed hydronephrosis with marked dilation of the renal pelvis, due to a reversible obstruction of the ureter cannula.

Ischemia-reperfusion injury (IRI) is an important determinant of deceased-donor organ functionality. We induced a standardized amount of ischemic injury to a section of the kidney by temporarily inflating a balloon catheter in one of the main branches of the renal artery, followed by deflation which resulted in reperfusion. With ischemia times ranging from 30 to 90 min, a T2-weighted MRI of these porcine kidneys provided us with an imaging biomarker reflecting ischemic changes and tissue recovery during reperfusion. During ischemia, the T2 signal became notably lower and after reperfusion, it took up to 30 min for this signal to recover to its initial value (Figure 2D–F). These experimental observations proved to possess clinical diagnostic relevance once we included discarded human donor kidneys in our studies. In the first experiment using a human kidney, a well-demarcated spontaneous ischemic area appeared on T2-weighted images, visually comparable to induced IRI in our porcine experiments (Figure 2G). The presence of this ischemic area was not noted during surgical organ inspection, nor could it be discerned macroscopically prior to or after the start of perfusion. Re-inspection after completion of the experiment revealed an unintentionally transected arterial branch of the upper pole.

TABLE 1 Summary of experiments per MRI acquisition

MRI acquisition	Applied and optimized	Protocolled experiments	Summary results
T2-weighted imaging	Porcine <i>n</i> = 22 Human <i>n</i> = 4	Induced ischemia-reperfusion (duration 30–90 min) Porcine <i>n</i> = 6 Iron oxide labeled MSCs Porcine <i>n</i> = 1	During ischemia, the T2 signal notably decreased and after reperfusion, it took up to 30 min for this signal to recover to its initial value. MSCs were inhomogeneously deposited within the renal cortex
T2* map	Porcine <i>n</i> = 22 Human <i>n</i> = 4	Deoxygenation 20 min Porcine <i>n</i> = 1	Baseline: T2* = 50.4 ms 5 min stop O <sub>2</sub> : T2* = 46.2 ms 10 min stop O <sub>2</sub> : T2* = 47.8 ms 20 min stop O <sub>2</sub> : T2* = 27.8 ms 5 min restart O <sub>2</sub> : T2* = 45.3 ms
ASL	Porcine <i>n</i> = 13	Perfusion maps first 3 h Porcine <i>n</i> = 9 Human <i>n</i> = 4	Corticomedullar ratio at 30, 60, 120, and 180 min Porcine: 2.1, 5.0, 6.5 and 5.3 Human: 1.2, 3.0, 4.5 and 6.6
Spectroscopy	<i>n.a.</i>	Hyperpolarized [1- <sup>13</sup> C]pyruvate Porcine <i>n</i> = 4	<sup>13</sup> C-lactate concentrations were decreased in the cortex compared with the medullar regions

Abbreviations: ASL, arterial spin labeling; MRI, magnetic resonance imaging; MSCs, mesenchymal stromal cells.

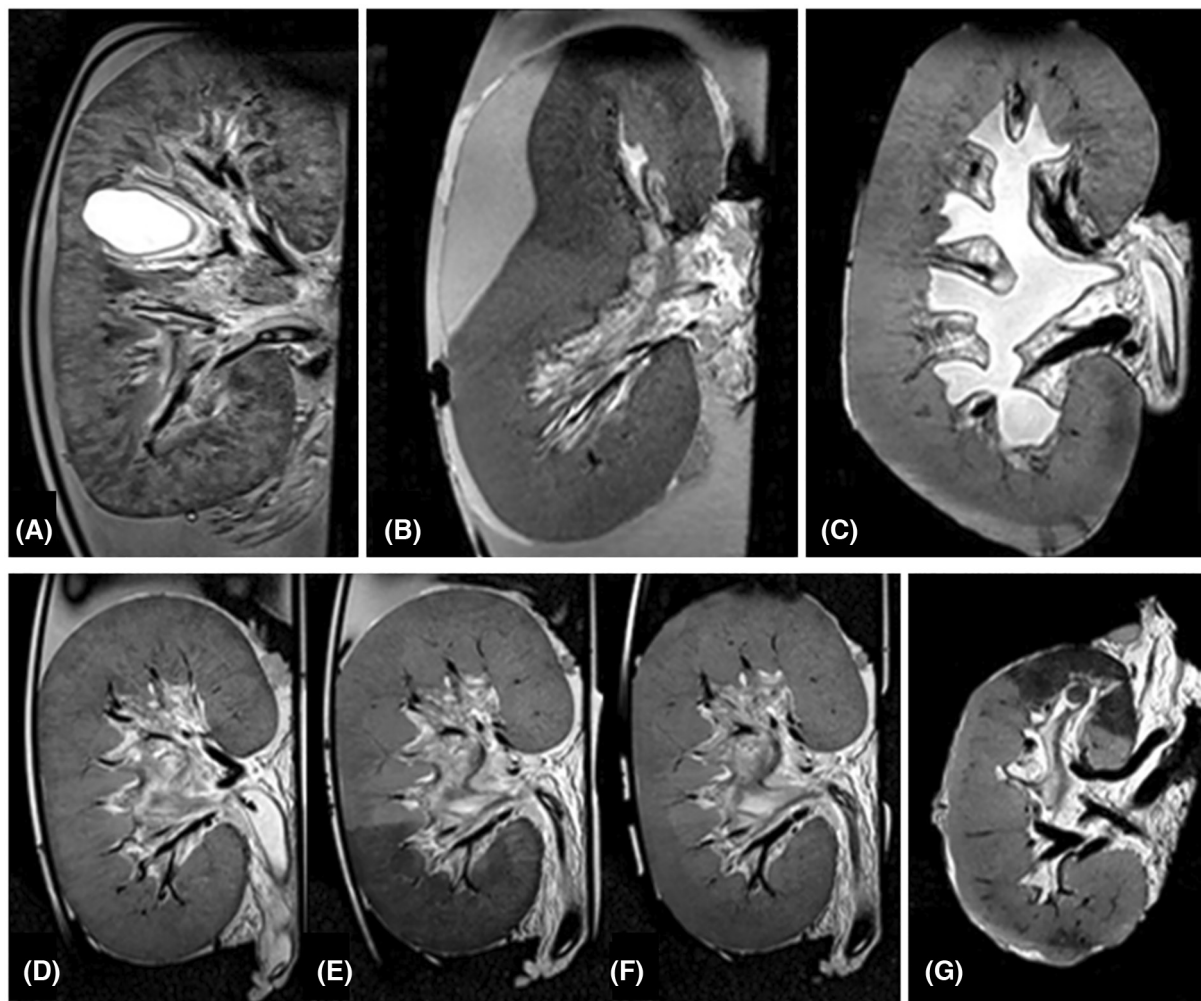


**FIGURE 2** T2-weighted images of structural abnormalities and ischemia/reperfusion damage. (A) Renal cyst not visible by visual inspection of the kidney's surface. (B) Subcapsular hematoma compressing part of the parenchyma and large intrarenal vessels. (C) Hydronephrosis due to an external obstruction of the ureter cannula. (D–F) Porcine kidney without ischemia, 60 min after induced partial ischemia (segmental area with lower T2 signal) and 30 min after reperfusion (segmental T2 signal almost recovered to its initial intensity). (G) Human discarded kidney (without intervention) with regional perfusion defect only visible on MRI.

### 3.2 | Regional perfusion

Intrarenal flow distribution and its evolution in time can neither be characterized by visual inspection, nor by measuring total renal flow with an external flow sensor in the NMP circuit. Regional flow distribution was measured with a standardized perfusion and imaging protocol in nine porcine and four discarded human kidneys by means of arterial spin labeling (ASL). ASL is a contrast-free functional MRI technique that enables the quantification of regional intrarenal blood or perfusate flow. Inflowing perfusate in the renal artery was labeled with radiofrequency pulses and, thus, the labeled fluid acted as an endogenous contrast agent. Using detailed ASL-based perfusion maps of each kidney at standardized time points, we were able to visualize regional flow distribution during ex vivo

reperfusion over time and compare this distribution between porcine and human kidneys.

To quantify intrarenal flow distribution, a cortico-medullar (CM) ratio was calculated from the ASL perfusion maps. By means of overlaying coronal T2-weighted anatomical images and ASL perfusion maps, regions of interest (ROIs) were drawn corresponding to the cortical area and the medullar pyramids (Figure 3A–C). The mean CM ratios in porcine kidneys after 30, 60, 120, and 180 min were 2.1, 5.0, 6.5, and 5.3, respectively and in human discarded kidneys 1.2, 3.0, 4.5, and 6.6 (Table 2). Furthermore, we observed a heterogeneous relation between the externally measured renal perfusate flow and the CM ratio derived from ASL perfusion maps. Some kidneys with a very stable perfusate flow during the entire experiment showed clearly increasing CM ratios over time.

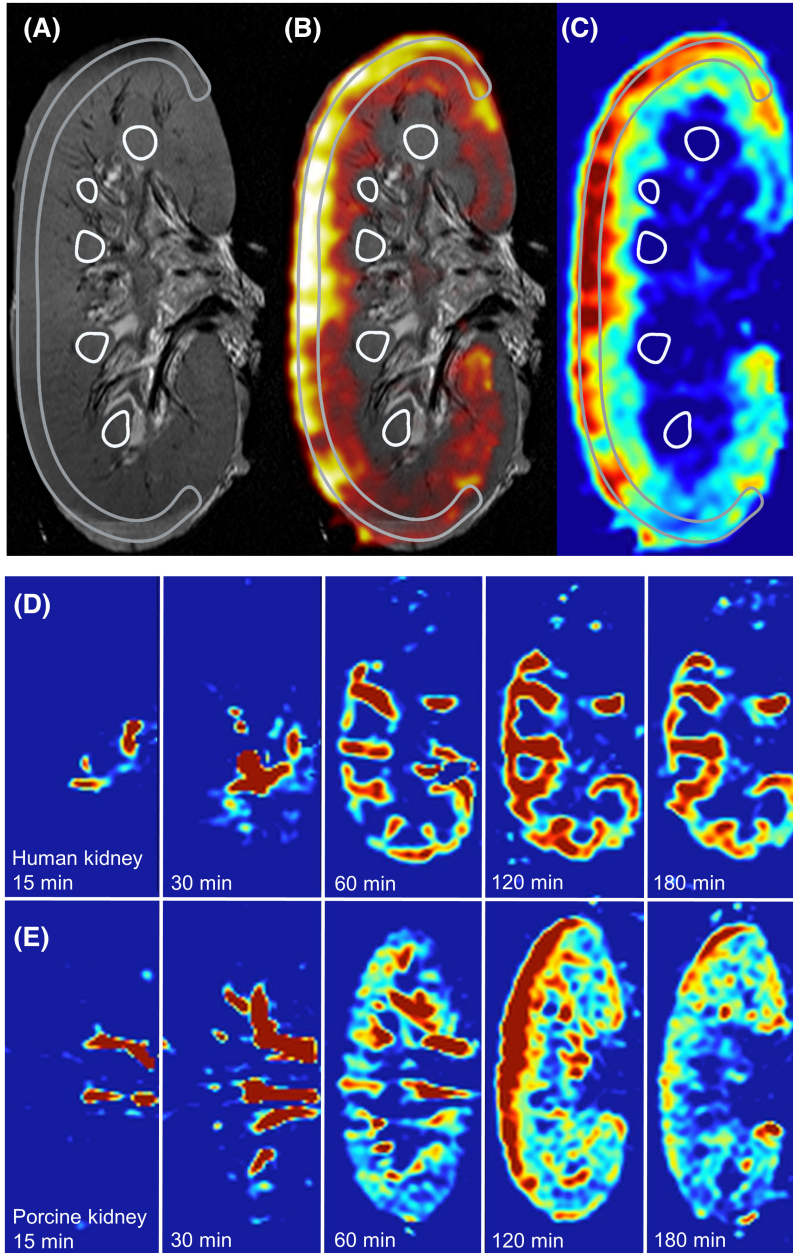


**FIGURE 3** ASL-derived perfusion maps. Adopted from Schutter et al.<sup>18</sup> (A) T2-weighted anatomical image with a C-shaped cortical region of interest (ROI) and several medullary ROIs drawn. (B) Overlay of T2 and ASL perfusion map. (C) ASL-derived perfusion map in which corticomedullary ratio was calculated utilizing the ROIs that were drawn on the anatomical image. Red areas indicate a high and blue a low flow rate of the perfusate in the kidney. (D) ASL-derived perfusion map of a human discarded kidney after 15, 30, 60, 120, and 180 min of NMP. (E) ASL-derived perfusion map of a porcine kidney after 15, 30, 60, 120, and 180 min of NMP. [Color figure can be viewed at [wileyonlinelibrary.com](http://wileyonlinelibrary.com)]

### 3.3 | Renal oxygen availability and metabolism

Functional MRI has the potential to characterize and quantify metabolic processes in real time that cannot be objectified by direct visual inspection of the organ or measurement of NMP hemodynamic parameters. Contrast in acquisitions using T2\* weighted imaging is affected by deoxygenated hemoglobin (deoxy-Hb), a paramagnetic hemoglobin species.<sup>9</sup> We evaluated the effect of oxygen depletion in kidneys perfused with continuous pressure of 85 mm Hg with a stable renal perfusate flow. The perfusion solution was oxygenated with 0.5 L/min carbogen gas (95% O<sub>2</sub> + 5% CO<sub>2</sub>), paused for 20 min, and then resumed with the same gas flow rate. The T2\* maps show

how regional differences in oxygen availability changed over time (Figure 4A–E). As oxygen consumption by the organ continued, deoxy-Hb accumulated which resulted in a lower T2\* signal. An ROI was drawn covering the whole kidney, resulting in T2\* values of 50.4 ms at baseline, 27.8 ms after pausing the oxygen supply for 20 min, and 45.3 ms 5 min after restarting oxygenation.

Another promising tool for evaluating ex vivo renal metabolism is MR spectroscopy (MRS). We injected hyperpolarized [1-<sup>13</sup>C]pyruvate into ex vivo perfused porcine kidneys. MRI combined with MRS of these kidneys provided highly detailed information on renal metabolism and its regional distribution.<sup>10</sup> After the injection of [1-<sup>13</sup>C] pyruvate in the arterial line near the renal artery, it enters the kidney and distributes into the tissue (Figure 4F,G).

**TABLE 2** Perfusion characteristics of porcine and human kidneys

Minutes after the start of NMP	Porcine kidneys <i>n</i> = 9	Human kidneys <i>n</i> = 4
	Mean (SD)	Mean (SD)
Mean externally measured flow (ml/min/100 g)		
30	83 (±39)	143 (±66)
60	117 (±31)	185 (±90)
120	129 (±51)	226 (±68)
180	116 (±46)	244 (±50)
ASL signal ratio (cortex/medulla)		
30	2.1 (±2.1)	1.2 (±1.0)
60	5.0 (±5.0)	3.0 (±1.1)
120	6.5 (±6.4)	4.5 (±1.0)
180	5.3 (±3.7)	6.6 (±2.8)

Source: Adopted from Schutter et al.<sup>18</sup>

Abbreviations: ASL, arterial spin labeling; NMP, normothermic machine perfusion.

The enzymatic conversion of [<sup>1-13</sup>C]pyruvate to lactate indicates anaerobic metabolism, whereas bicarbonate is produced under aerobic conditions. <sup>13</sup>C-lactate concentrations were decreased in the cortex compared with the medullar regions (Figure 4H,I), giving a unique insight into ex vivo intrarenal metabolism distribution.

### 3.4 | Therapeutic tracing

In addition to pre-transplant organ evaluation, NMP offers the opportunity to administer pharmacological or cellular therapy to the organ prior to transplantation. We investigated whether MRI can serve as a tool to monitor the distribution of ex vivo cellular therapy, such as with mesenchymal stromal cells (MSCs). One million human bone-marrow-derived MSCs were labeled with FeraTrack® (Miltenyi Biotec, Bergisch Gladbach, Germany) and infused into the arterial line of the perfusion circuit. T2 weighted imaging, performed before and after administration of the labeled MSCs, showed areas with a high concentration of infused cells and an intrarenal distribution which suggests that MSCs were inhomogeneously deposited within the renal cortex (Figure 5).<sup>11</sup>

## 4 | DISCUSSION

Although MRI assessment of ex vivo normothermic perfused organs is currently still in a developmental phase, our data suggest that the method is feasible and has the potential to add new diagnostic and investigational tools

to the fields of organ transplantation, renal physiology, and radiology. Some structural abnormalities, as well as perfusion and other functional parameters of a donor organ, can also be visualized in vivo in the donor with ultrasound, computed tomography, or MRI. Still, the damage that has accumulated after the donor's circulatory arrest, during organ procurement, and throughout the hours of cold organ preservation will only be visible in an ex vivo setting. We were able to identify an unexpected ischemic area in one of the discarded human kidneys, due to an iatrogenic dissected small arterial branch. Clinically, such a finding might have prompted either arterial reconstruction or kidney discard if reconstruction would not be possible.

Despite considerable efforts directed at developing NMP as an organ assessment platform, the important question of *what* to assess while a kidney is on the pump still remains. No validated sets of on-pump viability markers exist. Hence, in current clinical practice, most NMP markers are compared to in vivo references.

Several in vivo ASL studies have reported renal CM flow ratios between 5 and 7 in healthy volunteers, while patients with chronic kidney disease generally had a lower CM ratio.<sup>12,13</sup> CM ratios that we observed in porcine and human kidneys after 3 h of NMP are within the healthy physiological in vivo range.<sup>13-17</sup> These ASL measurements provide potentially viability-related information on the extent to which intrarenal flow distribution is in line with normal physiology. Since the majority of functional nephrons are located in the renal cortex, assessment of cortical perfusion could characterize important aspects of organ quality during perfusion. Given our data, the timing of such assessment should be carefully considered, since during the first 2-3 h after the start of NMP intrarenal flow distribution does not yet resemble normal in vivo physiology.<sup>18</sup> Medullar perfusion measured by ASL is reported to be less reproducible compared to cortical perfusion. Possible reasons are a reduced signal-to-noise ratio because of the relatively low medullar perfusion rate, incorrect segmentation of the medullar pyramids, and signal loss due to a longer transit time of the magnetically labeled fluid bolus which passes the cortex first.<sup>19</sup>

Magnetic resonance imaging during NMP also offers unique opportunities for more fundamental studies of organ metabolism and physiology. In their hypothermic perfusion model, Buchs et al demonstrated that adenosine triphosphate (ATP) levels could be detected in porcine kidneys by <sup>31</sup>P magnetic resonance spectroscopy and they also applied gadolinium contrast to measure intrarenal perfusion.<sup>20,21</sup> In 2020, in a hypothermic porcine model, it was found that ATP was rapidly generated in presence of oxygen and that warm ischemia reduced ATP levels, but not its precursors (AMP). ATP levels were inversely

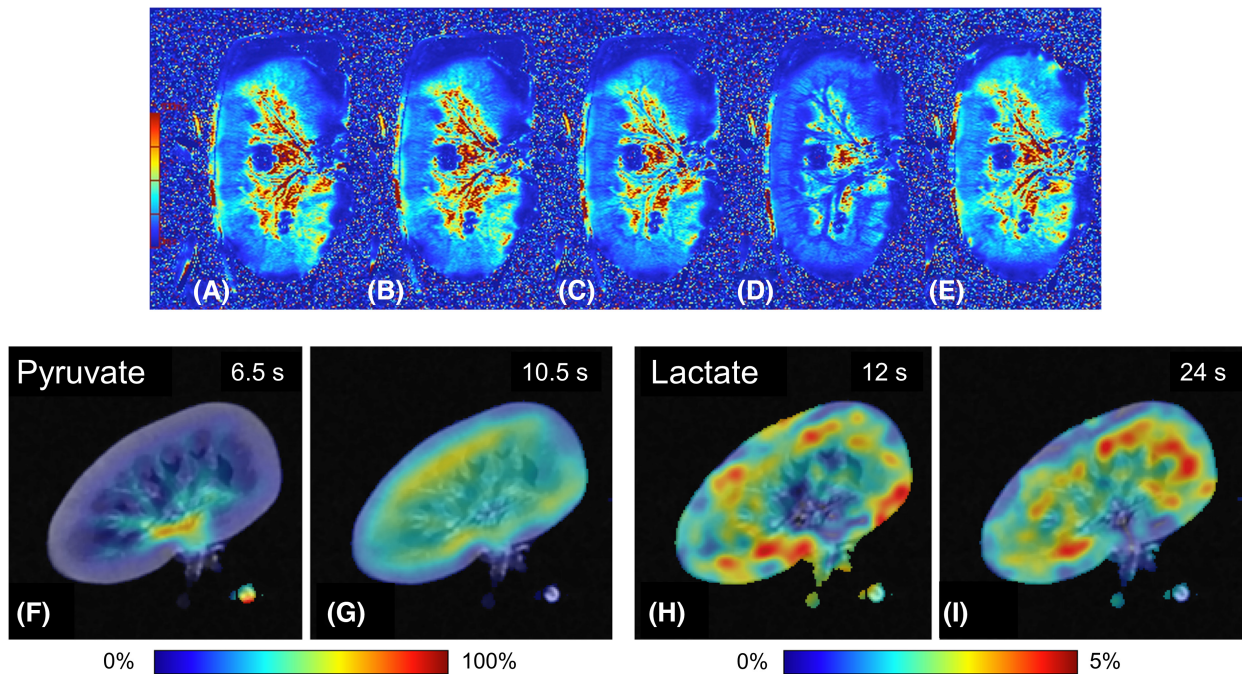


**FIGURE 4** Renal metabolism imaging. (A–E):  $T_2^*$  map showing regional differences in oxygen availability in a porcine kidney, approximately 5 h after the start of NMP. Increased concentrations of deoxygenated Hb cause a reduced  $T_2^*$  signal. Perfusion in this series was with continuous pressure of 85 mm Hg. This series highlights that it takes time for deoxygenated Hb to accumulate after cessation of oxygenation and that Hb is rapidly re-oxygenated when oxygen supply is resumed. (A) baseline perfusion (190 ml/min), oxygenated with carbogen (95%  $O_2$ /5%  $CO_2$ ) at a rate of 0.5 ml/min.  $T_2^* = 50.4$  ms. (B) 5 min after stopping the carbogen supply, perfusion 185 ml/min.  $T_2^* = 46.2$  ms. (C) 10 min after stopping the carbogen supply, perfusion 179 ml/min.  $T_2^* = 47.8$  ms. (D) 20 min after stopping the carbogen supply, perfusion 202 ml/min.  $T_2^* = 27.8$  ms.  $T_2^*$  signal is clearly reduced due to the increased deoxygenated Hb because of the oxygen consumption without supply. (E) 5 min after the restart of carbogen supply, perfusion 214 ml/min, rapidly leading to less deoxygenated Hb.  $T_2^* = 45.3$  ms. (F–I) Magnetic resonance spectroscopy providing information on lactate turnover using injected hyperpolarized [1- $^{13}C$ ] pyruvate in a porcine kidney. (F and G) the distribution of the hyperpolarized pyruvate tracer 6.5 and 10.5 s after the start of injection. (H and I) Signal intensities of the  $^{13}C$  lactate, 12 and 24 s after the start of injection for lactate. [Color figure can be viewed at [wileyonlinelibrary.com](http://wileyonlinelibrary.com)]

correlated with the severity of kidney histological injury, and could thus play an important role in assessing organ quality.<sup>22</sup>

The interaction between renal perfusion, glomerular filtration, oxygen delivery, and oxygen consumption is complex.<sup>14,23</sup> Blood oxygen level-dependent (BOLD) imaging and  $T_2^*$  mapping are functional MRI techniques that can quantify changes in regional oxygen availability. Our results showed that the  $T_2^*$  signal declines in the functionally important cortical area after cessation of oxygen supply. This could be a promising imaging biomarker for organ viability. Although arterial and venous blood gas samples might be of help in assessing the overall oxygen consumption of an organ during ex vivo perfusion,  $T_2^*$  functional imaging can provide rapid insight into intrarenal regional oxygen delivery and highlight areas with reduced or absent oxygenation. Several in vivo studies have demonstrated changes in tissue oxygen bioavailability during allograft dysfunction *after* transplantation.<sup>24–27</sup> In an ex vivo model with healthy kidneys, it might be possible

to detect where kidneys under NMP conditions touch on the scale of normal physiological oxygen consumption versus pathological ranges. Once normal values have been established, the same approach could be utilized to quantify the extent of organ dysfunction in potentially injured donor organs *before* transplantation.

Our newly developed platform also provides a tool to monitor ex vivo delivery of cellular or pharmacological therapies to injured donor kidneys, for example, the distribution of ex vivo infused iron-labeled mesenchymal stem cells. Apart from pharmacological interventions focused on organ quality improvement for transplantation, this platform also provides benefits for the general investigation of the pharmacokinetics of newly developed drugs in an isolated target organ. Furthermore, opportunities arise to safely test the targeted delivery of experimental labeled radioactive particles for intra-organ brachytherapy or visualize the uptake of MRI-visible organ-specific chemotherapeutic substances in an experimental setting.



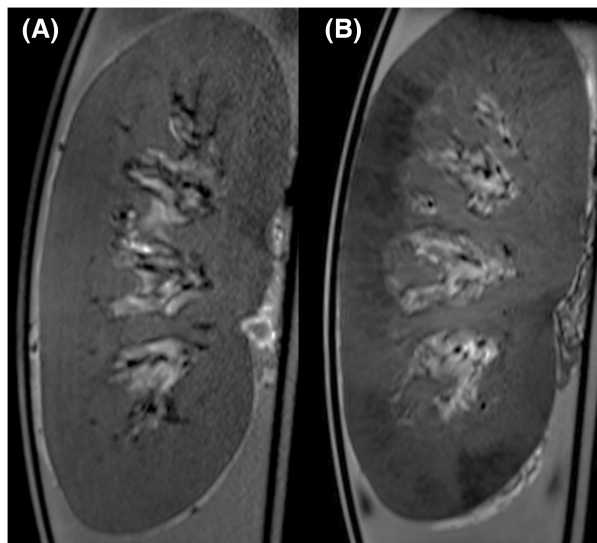


**FIGURE 5** Therapeutic tracing of mesenchymal stromal cells. Adopted from Pool et al.<sup>16</sup> (A) Baseline T2-weighted anatomical image of a porcine kidney during normothermic ex vivo perfusion (coronal view). (B) Same kidney after infusion of 1 million FeraTrack® labeled MSCs, manifesting as the dark areas in the renal cortex.

Although our studies already explored multiple MRI sequences, additional magnetic resonance acquisition methods could make a significant contribution to the future assessment of presumably suboptimal donor kidneys. Currently, the detection and quantification of relevant parenchymal pathology such as interstitial fibrosis, a strong predictor of long-term graft survival,<sup>28</sup> requires an invasive diagnostic needle biopsy. Yet, application of this gold standard procedure is limited due to risks of serious complications and the very small amount of tissue that can be obtained, which may not reflect the condition of the whole organ and makes these biopsies susceptible to sampling error.<sup>29–33</sup> Advances in MRI techniques, such as diffusion-weighted imaging and elastography, have created innovative opportunities to characterize renal scarring through imaging of distinct physical features of fibrotic and non-fibrotic tissue.<sup>34</sup> In addition, we foresee that ex vivo multiparametric MRI, providing imaging biomarkers that reflect different aspects of tissue structure and metabolism in one single acquisition, could be valuable in the quest to make pre-transplant organ quality assessment more objective, reliable, and very rapid.

Another relevant facet of MRI-compatible ex vivo organ perfusion is testing and validating novel renal MRI acquisition methods. Compared to in vivo imaging of healthy volunteers, ex vivo imaging of an isolated perfused organ is not influenced by motion artifacts. The ex vivo model also benefits from higher signal-to-noise ratios, with higher desired signals and lower levels of background noise. For example, the practical potential of the

new 3D imaging technique magnetic particle imaging angiography was tested in an ex-vivo hypothermic perfused kidney and could be compared with existing techniques.<sup>35</sup> It is likely that during warm perfusion, potential new applications can be tested more accurately, as the physiological setting is more similar to in vivo conditions. Moreover, our ex vivo method facilitates studying what certain imaging biomarkers indicate, by adjusting key input of variables such as perfusion pressure, oxygenation level, or hemoglobin concentration, which cannot be easily altered when imaging in vivo subjects.

An important limitation of this study is the purely descriptive nature, in which several MRI acquisitions have been tested in this newly developed experimental platform. At this developmental stage, our results have provided unique insights in renal physiology and metabolism, but it remains uncertain in which way these imaging markers will eventually convey clinically relevant metrics that predict graft function after transplantation.

Initial experiments on a limited number of porcine and discarded human kidneys were mainly focused on testing promising anatomical and functional MRI sequences. We evaluated their reproducibility and critically appraised the potential clinical translation of the type of data generated by each sequence. A fair comparison between porcine and discarded human kidneys included in our studies cannot be made, given the relevant differences in species, weight, age, and medical history. Human discarded kidneys had different warm and cold ischemia times depending on the type of donation procedure as well as logistics and were discarded for various medical reasons. In addition, the number of included human kidneys in this study is limited and more such experiments will be needed to fully translate our porcine results to the human setting.

Although MRI acquisition during isolated organ perfusions has a multifaceted range of applications, several hurdles should be overcome. The wide variety of clinical MRI scanners available makes it difficult to compare results between scanners, as even data from scanners from the same manufacturer are sensitive to differences due to circumstantial influences (e.g., shimming, inter-observer variability, protocol differences). This is a well-known culprit within the field of magnetic resonance imaging, but manufacturers are working on algorithms that can convert data to make measurements comparable between different scanners.

Moreover, if this technique will be clinically implemented, having a dedicated team performing the perfusion and operating the MRI is costly. As the current studies were all experimental and outside clinical “office hours,” actual costs are difficult to estimate in this early developmental phase. Due to the technical and logistical complexity, it would be recommended to first implement this method in



centers with extensive experience with organ perfusion. Protocolled consecutive acquisitions could be performed by an MRI technician on-site, while dedicated radiologists can report on the images from behind their desks. Actual costs will highly depend on arrangements that can be made with the radiology department and the use of staff that is “already” on call for organ perfusion procedures or general MRI staffing. However, this technique is still in its developmental phase and future cost-effectiveness evaluations might be necessary before clinical application.

The concept of applying magnetic resonance imaging during renal normothermic machine perfusion is novel in both renal and radiological research. With this new method, we have been able to obtain a detailed real-time view of ongoing processes *inside* human-sized kidneys while being perfused *ex vivo*. This platform allows for advanced pre-transplant organ assessment, provides a new realistic tool for studies into renal physiology and metabolism, and may serve as an ideal setup for MRI sequence development. Possible applications are numerous and our approach can easily be adapted to accommodate other organs as well. Our center has for example already successfully performed several pilot experiments with MRI during *ex-vivo* normothermic machine perfusion in discarded human livers.

Future perspectives could include protocolled imaging and perfusion experiments, in which clinically relevant variables (such as warm ischemia time, renal perfusion, or renal oxygenation levels) are accurately related to imaging markers. Multiomics and artificial intelligence might be able to better predict organ quality, in which imaging biomarkers will be one set of variables. Long-term perspectives include the development of a non-tethered, fully MRI-compatible NMP device, which could be used for non-invasive pre-transplant organ quality assessment. This would simplify the logistical process, allowing a more realistic period for clinical pre-transplantation quality assessment. In the near future, this new method could play a decisive role in donor organ quality assessment and allograft reconditioning.

## AUTHORS' CONTRIBUTIONS

*Research design, data acquisition, data analysis, data interpretation, writing of the manuscript:* Rianne Schutter and Veerle A. Lantinga. *Research design, data acquisition, data interpretation, writing of the manuscript:* Otis C. van Varsseveld. *Research design, data acquisition:* Merel B. F. Pool and Tim H. Hamelink. *Data acquisition, data analysis:* Jan Hendrik Potze. *Research design, critical revision of the manuscript:* Henri G. D. Leuvenink. *Research design, data acquisition, data analysis, data interpretation,*

*critical revision of the manuscript:* Christoffer Laustsen and Ronald J. H. Borra. *Research design, data acquisition, data interpretation, critical revision of the manuscript:* Cyril Moers.

## ACKNOWLEDGMENTS

Dutch Kidney Foundation, grant number: 17OI01 (CM); European Research Council, grant number: 851368—PRE-IMAGE (CM).

## CONFLICT OF INTEREST

The authors declare no competing interests, potential conflicts of interest, or any financial or personal relationship with organizations that could potentially be perceived as influencing the described research.




## DATA AVAILABILITY STATEMENT

MRI data are not openly stored, but access is available upon request to the corresponding author.

## ETHICAL CONSIDERATION

We have complied with all relevant ethical regulations. According to Dutch law, permission from an ethics review committee is not required when a study involves human subjects who have passed away. The Dutch law on organ donation states that individuals who give permission for organ donation, automatically also provide consent for transplantation-related research with their organs if an organ is discarded, unless the person explicitly objected. For ethical reasons, however, permission was requested from the donors' relatives, and written consent was obtained. For the porcine model in the Netherlands, kidneys were procured from a local slaughterhouse, in accordance with all guidelines of the Dutch food safety authority. For the kidneys procured in Denmark, the institutional and national guide for the care and use of laboratory animals was followed.

## ORCID

Rianne Schutter  <https://orcid.org/0000-0001-9461-8060>  
 Veerle A. Lantinga  <https://orcid.org/0000-0002-6931-2825>  
 Christoffer Laustsen  <https://orcid.org/0000-0002-0317-2911>

## REFERENCES

1. Rao S, Ghanta M, Moritz MJ, Constantinescu S. Long-term functional recovery, quality of life, and pregnancy after solid organ transplantation. *Med Clin North Am.* 2016;100(3):613–29.
2. Seiler A, Klaghofer R, Ture M, Komossa K, Martin-Soelch C, Jenewein J. A systematic review of health-related quality of life and psychological outcomes after lung transplantation. *J Heart Lung Transplant.* 2016;35(2):195–202.
3. Emin A, Rogers CA, Banner NR, Steering Group UKCTA. Quality of life of advanced chronic heart failure: medical care, mechanical circulatory support and transplantation. *Eur J Cardiothorac Surg.* 2016;50(2):269–73.



4. Rajkumar T, Mazid S, Vucak-Dzumhur M, Sykes TM, Elder GJ. Health-related quality of life following kidney and simultaneous pancreas kidney transplantation. *Nephrology (Carlton)*. 2019;24(9):975–82.
5. Schnitzler MA, Lentine KL, Gheorghian A, Axelrod D, Trivedi D, L'Italien G. Renal function following living, standard criteria deceased and expanded criteria deceased donor kidney transplantation: impact on graft failure and death. *Transpl Int*. 2012;25(2):179–91.
6. Weissenbacher A, Vrakas G, Nasralla D, Ceresa CDL. The future of organ perfusion and re-conditioning. *Transpl Int*. 2019;32(6):586–97.
7. Moers C, Smits JM, Maathuis MH, Treckmann J, van Gelder F, Napieralski BP, et al. Machine perfusion or cold storage in deceased-donor kidney transplantation. *N Engl J Med*. 2009;360(1):7–19.
8. Buchs JB, Buhler L, Morel P. A new disposable perfusion machine, nuclear magnetic resonance compatible, to test the marginal organs and the kidneys from non-heart-beating donors before transplantation. *Interact Cardiovasc Thorac Surg*. 2007;6(4):421–4.
9. Chavhan GB, Babyn PS, Thomas B, Shroff MM, Haacke EM. Principles, techniques, and applications of T2\*-based MR imaging and its special applications. *Radiographics*. 2009;29(5):1433–49.
10. Mariager CO, Hansen ESS, Bech SK, Munk A, Kjaergaard U, Lyhne MD, et al. Graft assessment of the ex vivo perfused porcine kidney using hyperpolarized [1-(13) C]pyruvate. *Magn Reson Med*. 2020;84:2645–55.
11. Pool M, Eertman T, Sierra Parraga J, Hart N, Roemeling-van Rhijn M, Eijken M, et al. Infusing mesenchymal stromal cells into porcine kidneys during normothermic machine perfusion: intact MSCs can be traced and localised to glomeruli. *Int J Mol Sci*. 2019;20(14):3607.
12. Gillis KA, McComb C, Patel RK, Stevens KK, Schneider MP, Radjenovic A, et al. Non-contrast renal magnetic resonance imaging to assess perfusion and corticomedullary differentiation in health and chronic kidney disease. *Nephron*. 2016;133(3):183–92.
13. Haddock B, Larsson HBW, Francis S, Andersen UB. Human renal response to furosemide: Simultaneous oxygenation and perfusion measurements in cortex and medulla. *Acta Physiol (Oxf)*. 2019;227(1):e13292.
14. Evans RG, Ince C, Joles JA, Smith DW, May CN, O'Connor PM, et al. Haemodynamic influences on kidney oxygenation: clinical implications of integrative physiology. *Clin Exp Pharmacol Physiol*. 2013;40(2):106–22.
15. Artz NS, Sadowski EA, Wentland AL, Grist TM, Seo S, Djamali A, et al. Arterial spin labeling MRI for assessment of perfusion in native and transplanted kidneys. *Magn Reson Imaging*. 2011;29:74–82.
16. Gardener AG, Francis ST. Multislice perfusion of the kidneys using parallel imaging: image acquisition and analysis strategies. *Magn Reson Med*. 2010;63(6):1627–36.
17. Fenchel M, Martirosian P, Langanke J, Giersch J, Miller S, Stauder NI, et al. Perfusion MR imaging with FAIR true FISP spin labeling in patients with and without renal artery stenosis: initial experience. *Radiology*. 2006;238(3):1013–21.
18. Schutter R, Lantinga VA, Hamelink TL, Pool MBF, van Varsseveld OC, Potze JH, et al. Magnetic resonance imaging assessment of renal flow distribution patterns during ex vivo normothermic machine perfusion in porcine and human kidneys. *Transpl Int*. 2021;34(9):1643–55.
19. Odudu A, Nery F, Hartevelde AA, Evans RG, Pendse D, Buchanan CE, et al. Arterial spin labelling MRI to measure renal perfusion: a systematic review and statement paper. *Nephrol Dial Transplant*. 2018;33(suppl\_2):ii15–21.
20. Lazeyras F, Buhler L, Vallee JP, Hergt M, Nastasi A, Ruttimann R, et al. Detection of ATP by “in line” 31P magnetic resonance spectroscopy during oxygenated hypothermic pulsatile perfusion of pigs' kidneys. *MAGMA*. 2012;25(5):391–9.
21. Buchs JB, Buehler L, Moll S, Ruttimann R, Nastasi A, Kasten J, et al. DCD pigs' kidneys analyzed by MRI to assess ex vivo their viability. *Transplantation*. 2014;97(2):148–53.
22. Longchamp A, Klauser A, Songeon J, Agius T, Nastasi A, Ruttimann R, et al. Ex vivo analysis of kidney graft viability using 31P magnetic resonance imaging spectroscopy. *Transplantation*. 2020;104(9):1825–31.
23. Evans RG, Gardiner BS, Smith DW, O'Connor PM. Intrarenal oxygenation: unique challenges and the biophysical basis of homeostasis. *Am J Physiol Renal Physiol*. 2008;295(5):F1259–70.
24. Han F, Xiao W, Xu Y, Wu J, Wang Q, Wang H, et al. The significance of BOLD MRI in differentiation between renal transplant rejection and acute tubular necrosis. *Nephrol Dial Transplant*. 2008;23:2666–72.
25. Sadowski EA, Djamali A, Wentland AL, Muehrer R, Becker BN, Grist TM, et al. Blood oxygen level-dependent and perfusion magnetic resonance imaging: detecting differences in oxygen bioavailability and blood flow in transplanted kidneys. *Magn Reson Imaging*. 2010;28:56–64.
26. Liu G, Han F, Xiao W, Wang Q, Xu Y, Chen J. Detection of renal allograft rejection using blood oxygen level-dependent and diffusion weighted magnetic resonance imaging: a retrospective study. *BMC Nephrol*. 2014;15:158.
27. Park SY, Kim CK, Park BK, Kim SJ, Lee S, Huh W. Assessment of early renal allograft dysfunction with blood oxygenation level-dependent MRI and diffusion-weighted imaging. *Eur J Radiol*. 2014;83:2114–21.
28. Ellingsen AR, Jorgensen KA, Osterby R, Petersen SE, Juul S, Marcussen N, et al. Human kidney graft survival correlates with structural parameters in baseline biopsies: a quantitative observational cohort study with more than 14 years' follow-up. *Virchows Arch*. 2021;478(4):659–68.
29. Fang J, Li G, Xu L, Zhang L, Yin W, Lai X, et al. Complications and clinical management of ultrasound-guided renal allograft biopsies. *Transl Androl Urol*. 2019;8(4):292–6.
30. Redfield RR, McCune KR, Rao A, Sadowski E, Hanson M, Kolterman AJ, et al. Nature, timing, and severity of complications from ultrasound-guided percutaneous renal transplant biopsy. *Transpl Int*. 2016;29(2):167–72.
31. Preda A, Van Dijk LC, Van Oostaijen JA, Pattynama PM. Complication rate and diagnostic yield of 515 consecutive ultrasound-guided biopsies of renal allografts and native kidneys using a 14-gauge Biopty gun. *Eur Radiol*. 2003;13(3):527–30.
32. Mahoney MC, Racadio JM, Merhar GL, First MR. Safety and efficacy of kidney transplant biopsy: Tru-Cut needle vs sonographically guided Biopty gun. *AJR Am J Roentgenol*. 1993;160(2):325–6.
33. Solez K, Racusen LC. The Banff classification revisited. *Kidney Int*. 2013;83(2):201–6.
34. Leung G, Kirpalani A, Szeto SG, Deeb M, Foltz W, Simmons CA, et al. Could MRI be used to image kidney fibrosis? a review of recent advances and remaining barriers. *Clin J Am Soc Nephrol*. 2017;12(6):1019–28.



35. Molwitz I, Ittrich H, Knopp T, Mummert T, Salamon J, Jung C, et al. First magnetic particle imaging angiography in humanized organs by employing a multimodal ex vivo pig kidney perfusion system. *Physiol Meas*. 2019;40(10):105002.

### SUPPORTING INFORMATION

Additional supporting information can be found online in the Supporting Information section at the end of this article.

**How to cite this article:** Schutter R, van Varsseveld OC, Lantinga VA, Pool MBF, Hamelink TH, Potze JH, et al. Magnetic resonance imaging during warm ex vivo kidney perfusion. *Artif. Organs*. 2023;47:105–116. <https://doi.org/10.1111/aor.14391>